Inclusive π^0 Production at Large Transverse Momentum from $\pi^{\pm}p$ and pp Interactions at 100 and 200 GeV/c*

G. Donaldson, H. Gordon, K.-W. Lai, and I. Stumer
Brookhaven National Laboratory, Upton, New York 11973

and

A. Barnes, J. Mellema, A. Tollestrup, and R. Walker
California Institute of Technology, Pasadena, California 91109

and

O. Dahl, R. A. Johnson, A. Ogawa, M. Pripstein, and S. Shannon
Lawrence Berkeley Laboratory, Berkeley, California 94720

(Received 10 February 1976)

We have measured large-transverse-momentum ($p_\perp$) inclusive π^0 production at c.m. angles centered near 90° for $\pi^{\pm}p$ and pp interactions at 100 and 200 GeV/c. This is the first such measurement using a pion beam. The ratio $\sigma(pp \to \pi^0 X)/\sigma(\pi p \to \pi^0 X)$ decreases with increasing $p_\perp$ and is independent of energy when expressed as a function of $x_\perp = p_\perp / p_{\max}$. We compare the data with predictions of various models.

Particle production at large transverse momentum ($p_\perp$) is believed to result from the interaction of hadronic constituents.[1] A variety of single-particle inclusive data from the CERN intersecting storage rings[2] and from Fermilab[3] have been described with some success in terms of this hypothesis, but all of these were measurements of proton-proton or proton-nucleus interactions. To investigate the possible role of hadronic constituents in large-$p_\perp$ particle production, it is important to compare reactions produced by different incident particles having different internal structures. We report here the first measurement of inclusive π^0 production at large $p_\perp$ using high-energy pion beams, and compare these results with proton-induced data obtained under the same conditions.

The experiment was performed in the $M2$ beam at Fermilab. The apparatus (shown schematically in Fig. 1) consisted of two helium-filled differential Čerenkov counters, a series of beam-defining counters, a 60-cm liquid-hydrogen target, and a photon detector.[4] Each of the Čerenkov counters was equipped with two phototubes which viewed two cones of light, thus allowing simultaneous π, K, and p identification. The beam-defining counters excluded beam halo and double beam particles as well as most upstream interactions. Two hodoscopes measured the position and direction of the incident particle. The photon detector, a lead-scintillator-sandwich hodoscope of 70 horizontal and 70 vertical counters, contains 19 radiation lengths of lead interspersed with long narrow (73.5×1.05 cm) scintillator rods. Each counter (a group of eight optically coupled rods) integrates the photon shower development along its direction of propagation. The hodoscope pulse heights give the transverse distributions of the energy deposited by all the photons hitting the detector.

The photon detector was displaced horizontally from the beam axis to have good acceptance for π^0's in a region of c.m. angles from 50° to 110°. For triggering purposes, a weighted analog sum of the pulse heights in the vertical counters of the detector was formed; this sum was roughly proportional to the total transverse momentum of the observed photons. When a sufficiently large $p_\perp$ event was indicated, the pulse heights in all 140 counters were recorded on magnetic tape. The gains of the phototubes were monitored continuously during the experiment to an accuracy of about 1%.

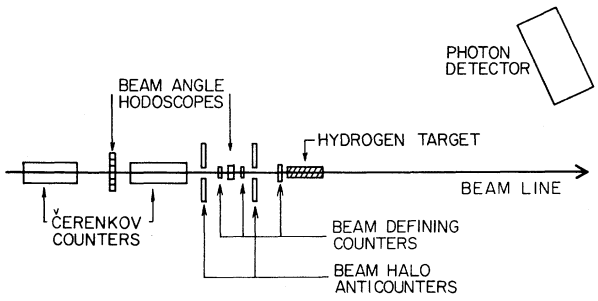

FIG. 1. Schematic view of apparatus—not to scale.

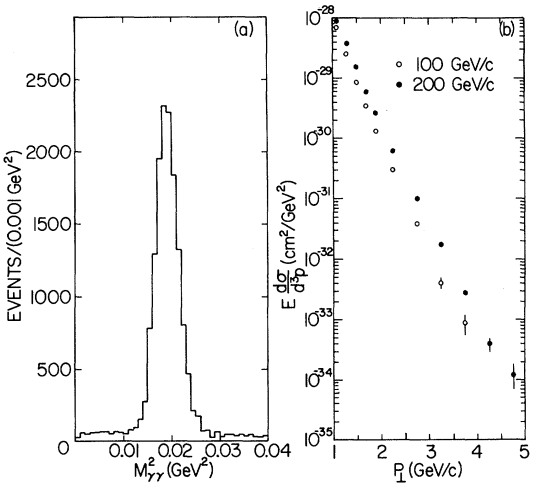

FIG. 2. (a) Mass spectrum of two-photon combinations for $2.0 < p_\perp < 2.5$ GeV/c from $\pi^- p$ interactions. For events with more than two photons in the detector, the pair with the largest $p_\perp$ is plotted. (b) The invariant cross section versus $p_\perp$ for the reaction $\pi^- p \to \pi^0 X$ at 100 and 200 GeV/c and c.m. angles near 90°.

By detailed off-line analysis of the pulse-height data, the position and energy of all photon showers in the detector were determined with a spatial resolution of ±1 mm and energy resolution $\Delta E/E \approx 0.02(100\ \text{GeV}/E)^{1/2}$. Since this was an inclusive measurement, an event candidate was not rejected if more than two showers appeared in the detector; rather the photon pair having the largest $p_\perp$ was selected.[5] The resulting pair mass spectrum shows a clean π^0 peak as illustrated in Fig. 2(a). The background is composed of unassociated pairs of photons and/or charged particles. Its magnitude is on the average about 10% of the π^0 signal, and has the same $p_\perp$ dependence as the π^0 signal for all initial states. The resolution in mass is $\Delta M^2/M^2 \approx 12\%$. The number of π^0's within a given $p_\perp$ interval was determined by fitting the mass spectrum for that interval (with target-empty contributions subtracted) with a Gaussian plus a linear background. The resulting invariant cross sections for $\pi^\pm p \to \pi^0 X$ and $pp \to \pi^0 X$ are given in Table I. In all three reactions the cross section at fixed $p_\perp$ increases with increasing beam energy as shown in Fig. 2(b) for $\pi^- p \to \pi^0 X$. The cross section for $pp \to \pi^0 X$ is consistent with previous experiments.[3]

The principal objective of this experiment is a measurement of the ratios

$$R\left(\frac{A}{B}\right) = \frac{E d\sigma(Ap \to \pi^0 X)/d^3p}{E d\sigma(Bp \to \pi^0 X)/d^3p},$$

where A and B are p, π^+, or π^-. Results were obtained for each different reaction using the same apparatus, running conditions, and analysis procedures so that this ratio would be insen-

TABLE I. Invariant cross sections $E(d\sigma/d^3p)$ (cm²/GeV²) at $\theta_{\text{c.m.}} = 90°$ for the reactions $Ap \to \pi^0 + X$ where $A = \pi^+$, π^-, and p.[a]

$p_\perp$ Interval (GeV/c)	100 GeV/c			200 GeV/c		
	π^+	π^-	p	π^+	π^-	p
1.0-1.2	$(6.53\pm0.52)\times10^{-29}$	$(6.70\pm0.54)\times10^{-29}$	$(1.12\pm0.09)\times10^{-28}$	$(9.78\pm0.78)\times10^{-29}$	$(9.09\pm0.73)\times10^{-29}$	$(1.31\pm0.10)\times10^{-28}$
1.2-1.4	$(2.72\pm0.22)\times10^{-29}$	$(2.59\pm0.21)\times10^{-29}$	$(4.02\pm0.32)\times10^{-29}$	$(3.71\pm0.30)\times10^{-29}$	$(3.77\pm0.30)\times10^{-29}$	$(5.92\pm0.47)\times10^{-29}$
1.4-1.6	$(1.04\pm0.83)\times10^{-29}$	$(8.57\pm0.69)\times10^{-30}$	$(1.25\pm0.10)\times10^{-29}$	$(1.62\pm0.13)\times10^{-29}$	$(1.49\pm0.12)\times10^{-29}$	$(2.13\pm0.17)\times10^{-29}$
1.6-1.8	$(3.72\pm0.30)\times10^{-30}$	$(3.41\pm0.27)\times10^{-30}$	$(4.92\pm0.39)\times10^{-30}$	$(6.44\pm0.52)\times10^{-30}$	$(5.95\pm0.48)\times10^{-30}$	$(8.82\pm0.71)\times10^{-30}$
1.8-2.0	$(1.55\pm0.12)\times10^{-30}$	$(1.44\pm0.12)\times10^{-30}$	$(1.86\pm0.15)\times10^{-30}$	$(3.16\pm0.25)\times10^{-30}$	$(2.59\pm0.21)\times10^{-30}$	$(3.86\pm0.31)\times10^{-30}$
2.0-2.5	$(3.46\pm0.28)\times10^{-31}$	$(3.07\pm0.25)\times10^{-31}$	$(3.98\pm0.32)\times10^{-31}$	$(5.93\pm0.47)\times10^{-31}$	$(6.22\pm0.50)\times10^{-31}$	$(8.57\pm0.69)\times10^{-31}$
2.5-3.0	$(3.93\pm0.31)\times10^{-32}$	$(3.83\pm0.31)\times10^{-32}$	$(2.77\pm0.23)\times10^{-32}$	$(1.21\pm0.10)\times10^{-31}$	$(9.72\pm0.78)\times10^{-32}$	$(1.23\pm0.10)\times10^{-31}$
3.0-3.5	$(4.24\pm0.60)\times10^{-33}$	$(4.0\pm0.6)\times10^{-33}$	$(2.20\pm0.64)\times10^{-33}$	$(1.81\pm0.23)\times10^{-32}$	$(1.76\pm0.14)\times10^{-32}$	$(1.57\pm0.13)\times10^{-32}$
3.5-4.0	$(5.21\pm3.0)\times10^{-34}$	$(8.6\pm3.1)\times10^{-34}$		$(2.19\pm0.43)\times10^{-33}$	$(2.68\pm0.21)\times10^{-33}$	$(2.20\pm0.18)\times10^{-33}$
4.0-4.5				$(9.0\pm3.0)\times10^{-34}$	$(3.80\pm0.83)\times10^{-34}$	$(2.42\pm0.80)\times10^{-34}$
4.5-5.0					$(1.27\pm0.58)\times10^{-34}$	

[a] The quoted error combines a point-to-point systematic uncertainty of 8% with the normal statistical contribution. Not included in the quoted error is an additional 5% uncertainty in overall normalization and an uncertainty of 3% in the $p_\perp$ scale.

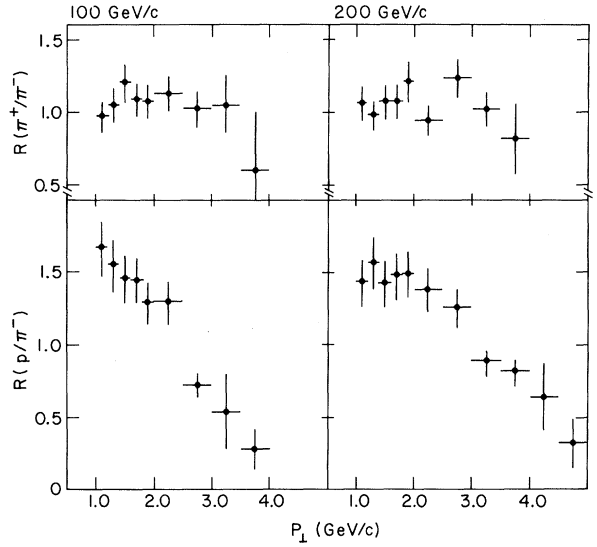

FIG. 3. Ratios of invariant cross sections as described in the text versus $p_\perp$.

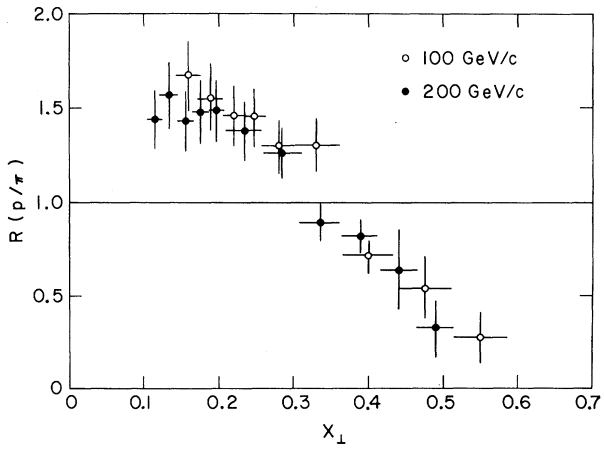

FIG. 4. Ratio of invariant cross sections versus $x_\perp$ for $pp \to \pi^0 X$ and $\pi^- p \to \pi^0 X$ at 100 and 200 GeV/c.

sitive to systematic errors affecting the individual cross sections; only the signature in the Čerenkov counters distinguished the reactions.[6]

The ratios $R(\pi^+/\pi^-)$ and $R(p/\pi^-)$ are presented in Fig. 3 as a function of $p_\perp$. At both 100 and 200 GeV/c, $R(\pi^+/\pi^-)$ is close to unity over the entire $p_\perp$ region investigated. In contrast, $R(p/\pi^-)$ changes markedly between $p_\perp \sim 1$ and $p_\perp \sim 4$ GeV/c. At $p_\perp \sim 1$ GeV/c, the ratio is about 1.6, which is equal to the ratio of the total pp and πp cross sections. This can be understood by factorization arguments in the Mueller-Regge theory[7] and has been observed before.[8] However, the ratio decreases with increasing $p_\perp$, falling to a point where the πp cross section significantly exceeds the pp cross section at the largest measured $p_\perp$. In the highest $p_\perp$ bin at each energy, a smooth extrapolation of our $pp \to \pi^0 + X$ data[9] was made in order to compute the ratio.

Although the value of $R(p/\pi^-)$ at a fixed $p_\perp$ is different at 100 and 200 GeV/c, $R(p/\pi^-)$ is independent of energy when expressed as a function of $x_\perp = p_\perp/p_{\max}$ as shown in Fig. 4. The pp and πp cross sections can be parametrized by a factorized function $Ed\sigma/d^3p \propto (p_\perp{}^2 + M^2)^N (1 - x_\perp)^F$. The best fit gives $N_p = -5.4 \pm 0.2$, $M_p{}^2 = 2.3 \pm 0.3$ GeV^2, $F_p = 7.1 \pm 0.4$ with χ^2 per degree of freedom $= \frac{23}{14}$ for $pp \to \pi^0 X$, and $N_\pi = -5.0 \pm 0.1$, $M_\pi{}^2 = 1.8 \pm 0.2$ GeV^2, $F_\pi = 5.5 \pm 0.3$ with χ^2 per degree of freedom $= \frac{44}{35}$ for $\pi^\pm p \to \pi^0 X$. In the context of this parametrization both πp and pp interactions have approximately the same $p_\perp$ dependence, and so the fall of $R(p/\pi)$ versus $x_\perp$ shown in Fig. 4 can be interpreted as the difference in the power of $(1 - x_\perp)$.

Under the assumption that large-$p_\perp$ π^0 production is dominated by quark-meson scattering ($qM \to qM$) or quark-antiquark annihilation ($q\bar{q} \to MM$) a simple application of the constituent interchange model[1] predicts $F_p - F_\pi = 6$, in disagreement with our measured result of 1.6 ± 0.5. Another parton model[10] of the "quark-fusion" type predicts a much smaller ratio $R(p/\pi)$ than is observed and hence is ruled out. If naively one thinks of the proton as having three constituents and the π as having two, then on the average the momentum of the constituents in the π should be larger than those in the proton. From this consideration alone one would expect that the probability to produce a π^0 at large $p_\perp$ would be somewhat larger for πp interactions than for pp interactions and that the difference between the two reactions should be in their $x_\perp$ rather than their $p_\perp$ dependence.

We would like to express our appreciation to Dr. R. Kenney for his continuing support and assistance throughout this experiment and to D. Hermeyer for his important contributions to the design and operation of the experiment. We gratefully acknowledge the cooperation of Dr. C. Brown and Dr. P. Koehler and many others at Fermilab.

*Work performed under the auspices of the U. S. Energy Research and Development Administration.

[1]For example: R. Blankenbeckler, S. C. Brodsky, and J. Gunion, SLAC Report No. SLAC-PUB-1585, 1975 (unpublished).

[2]For example: F. W. Büsser *et al.*, Phys. Lett. 46B, 471 (1973); M. Banner *et al.*, Phys. Lett. 44B, 537 (1973); B. Alper *et al.*, Phys. Lett. 44B, 521, 527 (1973).

[3]For example: D. C. Carey *et al.*, Phys. Rev. Lett. 33, 327 (1974); J. W. Cronin *et al.*, Phys. Rev. D 11, 3105 (1975); J. A. Appel *et al.*, Phys. Rev. Lett. 33, 719 (1974).

[4]The detector and other apparatus were used in a previous experiment on $\pi^- p$ charge exchange and are described in A. V. Barnes *et al.*, SLAC Report No. SLAC-179, 1974 (unpublished), Vol. I, p. 1; R. Johnson, Lawrence Berkeley Laboratory Report No. LBL-4610, 1975 (unpublished).

[5]Because of the steep falloff of the photon spectra with increasing $p_\perp$, we find that our neglect of the photon pairs with lower $p_\perp$ causes an error of less than 2% in the measured invariant cross sections.

[6]The contamination in the p and π^+ samples from misidentified particles is $\lesssim 0.5\%$. In the π^- sample the contamination is $\lesssim 0.1\%$.

[7]A. H. Mueller, Phys. Rev. D 2, 2963 (1970).

[8]J. Erwin *et al.*, Phys. Rev. Lett. 33, 1352 (1974).

[9]This extrapolation is consistent with the measurements in Refs. 2 and 3.

[10]B. L. Combridge, Phys. Rev. D 10, 3849 (1974).

Λ^0 Hyperon Polarization in Inclusive Production by 300-GeV Protons on Beryllium

G. Bunce, R. Handler, R. March, P. Martin, L. Pondrom, and M. Sheaff
Physics Department, University of Wisconsin, Madison, Wisconsin 53706*

and

K. Heller, O. Overseth, and P. Skubic
Physics Department,† University of Michigan, Ann Arbor, Michigan 48104

and

T. Devlin, B. Edelman, R. Edwards, J. Norem, L. Schachinger, and P. Yamin
Physics Department,† Rutgers University, New Brunswick, New Jersey 08903
(Received 1 December 1975)

Λ^0 polarization has been observed in $p + \mathrm{Be} \to \Lambda^0 +$ anything at 300 GeV. A total of 1.2×10^6 Λ^0 decays were recorded at fixed lab angles between 0 and 9.5 mrad, covering a range of kinematic variables $0.3 \leq x \leq 0.7$ and $0 \leq p_\perp \leq 1.5$ GeV/c. The observed polarization was consistent with parity conservation and increased monotonically with increasing $p_\perp$, independently of x, reaching $P_\Lambda = 0.28 \pm 0.08$ at 1.5 GeV/c.

Multiparticle-final-state reactions form the major part of the total cross section at high energies. The general case is difficult to treat both experimentally and theoretically because of the high multiplicity. Inclusive channels of the form $a + b \to c + X$, however, may be described in a fairly simple way because of the sum over the unobserved states X. There has been considerable experimental and theoretical activity in the study of kinematic distributions of inclusive channels for various choices of particles a, b, and c.[1] If any of these three particles has spin, then polarization effects are possible which furnish information sensitive to interference between various amplitudes contributing to the reaction. It is known that as the energy increases polarization effects in elastic scattering become very small.[2] Few measurements of high-energy inclusive polarization effects have been made.[3] This Letter reports the first observation of substantial polarization effects in inclusive production at 300 GeV. The polarization was observed in the channel $p + \mathrm{Be} \to \Lambda^0 + X$. A reaction of this type, where particle c is a Λ^0 hyperon, is particularly well suited to polarization measurements because the Λ^0 serves as its own spin analyzer through the decay $\Lambda^0 \to p + \pi^-$.[4]

Figure 1 shows the apparatus. The 300-GeV protons were deflected vertically (positive angles upwards) with a magnet 150 m upstream of the Λ^0 production target, and then restored to the target with magnets 5 m upstream, to obtain production angles between 0 and 9.5 mrad in a vertical plane. The neutral beam was defined by a fixed collimator with its axis in the horizontal plane. The collimator was 5.3 m long, compared to the decay length for 150-GeV/c Λ^0's of 10.4 m. A vertical magnetic field (the sweeping magnet) of 21 kG was applied to the collimator. A circular tungsten aperture 4 mm in diameter at 3.2 m defined